Structural, magnetic, and crystalline electric-field effects in single crystals of $Y_{1-x}Pr_xBa_2Cu_3O_{7-\delta}$

S. Uma, T. Sarkar, K. Sethupathi, M. Seshasayee, and G. Rangarajan
Department of Physics, Indian Institute of Technology, Madras 600 036, India

Chen Changkang, Hu Yongle, B. M. Wanklyn, and J. W. Hodby
Department of Physics, University of Oxford, Clarendon Laboratory, Oxford, 0X1 3PU United Kingdom
(Received 13 July 1995)

We report here structural and directional magnetic susceptibility measurements on single crystals of $Y_{1-x}Pr_xBa_2Cu_3O_{7-\delta}$ ($x=1.0$, $\delta=1$, 0.11; $x=0.7$, $\delta=0$; and $x=0.42$, $\delta=0.22$). The space group of $PrBa_2Cu_3O_6$ (Pr-O6) and $Y_{0.58}Pr_{0.42}Ba_2Cu_3O_{6.78}$ (Pr 0.42-O7) were found to be $P4/mmm$ and that of $PrBa_2Cu_3O_{6.89}$ (Pr-O7) was found to be $Pmmm$. Also, Pr-O7 was found to be weakly orthorhombic. Directional, magnetic susceptibility measurements in the temperature range 2–300 K revealed a clear peaking in the paramagnetic anisotropy of Pr-O7 around 17 K, and $\chi_c > \chi_{a,b}$ at all temperatures. However for $Y_{0.3}Pr_{0.7}Ba_2Cu_3O_7$ (Pr0.7-O7) and Pr0.42-O7, $\chi_c > \chi_{a,b}$ at room temperature and $\chi_c < \chi_{a,b}$ for temperatures below 110 and 60 K, respectively. The magnetic susceptibilities have been analyzed in the light of crystalline electric-field effects considering J mixing of all the thirteen multiplets. Intermediate coupled wave functions have also been used in the calculations. Crystal-field interaction is found to be stronger in the case of Pr-O7 compared to Pr-O6 which is also evident from a shorter Pr-O bond length in the case of Pr-O7 than in Pr-O6. A best set of eigenvalues and eigenfunctions has been determined and these are discussed and compared with inelastic neutron scattering data.

I. INTRODUCTION

The coexistence of superconductivity and magnetism in $RBa_2Cu_3O_{7-\delta}$ ($R=$ rare-earth ion) has been the subject of intense research over the last few years. Although a number of experimental results on the physical properties of this system have been reported, to date no single theory has been proposed explaining the superconducting behavior and its connection to magnetic properties. Of particular interest is the $Y_{1-x}Pr_xBa_2Cu_3O_{7-\delta}$ (YPBCO) system which exhibits a drastic suppression of the superconducting transition temperature (T_c) with Pr doping. Further, the antiferromagnetic ordering temperature of $PrBa_2Cu_3O_{7-\delta}$ (PBCO) has been found to be higher by two orders of magnitude compared to that of the other rare-earth ions.[1] Also, it has been reported that substitution of Pr in $YBa_2Cu_3O_{7-\delta}$ (YBCO) leads to an antiferromagnetic Néel temperature (T_N) which approximately increases linearly with the addition of Pr.[1] The saturation magnetic moment of Pr^{3+} ions as found from specific heat, susceptibility, and neutron diffraction experiments is $(0.74\pm0.08)\mu_B$ for $PrBa_2Cu_3O_7$ and $(1.9\pm0.2)\mu_B$ for $PrBa_2Cu_3O_6$. These values are small compared to the free-ion value of $3.58\mu_B$ for Pr^{3+} and $2.54\mu_B$ for Pr^{4+}. A calculation based on perfect three-dimensional long-range magnetic order yields neutron diffraction intensities which are nowhere near the measured values.[2,3]

With a belief that the unusual features exhibited by this system are due to the electronic properties of the $4f$ electrons, a number of experimental studies has been performed.[4–6] Of crucial importance are the low-lying electronic levels of the Pr^{3+} ion in this system, and until now there has been considerable controversy regarding their spacing and composition. Inelastic neutron scattering (INS) experiments on these compounds reveal that the ground state of the Pr^{3+} ion is composed of a quasitriplet of width less than 40 cm^{-1}, which is well separated from the remaining levels by about 500 cm^{-1}. Crystal-field (CF) analysis has been undertaken by most of these groups, and crystal-field parameters (CFP's) have been determined.[4–6] In addition, mean (powder) susceptibility (χ_{mn}) and specific heat measurements have also been carried out.[5,6] Most of the experimental results on this system have been limited to polycrystalline samples, and only a few measurements have been performed on well-characterized single crystals.[7–10]

The temperature dependence of the paramagnetic susceptibilities depends sensitively on the nature of the low-lying levels. Hence a study of the temperature dependence of the directional susceptibility and paramagnetic anisotropy was undertaken in the present work on single crystals of $Y_{1-x}Pr_xBa_2Cu_3O_{7-\delta}$. In this context it may be mentioned that there are already a few reports on x-ray diffraction studies on these compounds.[7,8] The main objective of our present study is to make a crystalline electric-field analysis of the magnetic susceptibilities and/or paramagnetic anisotropies. Crystalline electric fields act as a direct probe at the rare-earth site and sensitively depend on the symmetry, bond distances, and bond angles of the anions forming the environment of the rare-earth ion. This necessitated us to carry out a fresh x-ray diffraction study on the samples chosen for the present study so as to accurately determine the structural parameters and to compare them with the corresponding crystal-field parameters. We have therefore restricted our study to compositions whose Pr content is $0.4 \leqslant x \leqslant 1$ so as to

 © 1996 The American Physical Society

get maximum range of temperature of the susceptibility data for CF analysis.

II. EXPERIMENT

Single crystals of $Y_{1-x}Pr_xBa_2Cu_3O_{7-\delta}$ were grown by the flux method using polycrystalline YPBCO with a flux of BaO-CuO eutectic mixture. The crystals obtained were shiny black opaque platelets.[11,12]

A. Crystal structure measurements

Single-crystal x-ray diffraction data of PBCO and YPBCO were collected using an Enraf-Nonius CAD-4 diffractometer. Intensity data were collected by a ω-2θ scan technique for $2°<\theta<24°$ with graphite-monochromated Mo K_α ($\lambda=0.710\,69$ Å). 203 and 132 reflections with $I>3\sigma(I)$ were used for structure determination of the two samples, respectively. The structure was solved using the Patterson technique. An absorption correction was applied using the program ABSORB.[13] During the final cycles of refinement, the occupancy factors of the oxygens were varied. The final goodness of fit (S), shift/e.s.d., and R values were 1.103, 0.023, and 4.85 %, respectively, for PBCO, and those of YBPCO were 1.201, 0.374, and 2.44 %, respectively. The above analysis was carried out using the program SHELX-93.[14]

B. Magnetic susceptibility and paramagnetic-anisotropy measurements

Magnetic susceptibility measurements were performed on $PrBa_2Cu_3O_{7-\delta}$ (Pr-O7), $Y_{0.3}Pr_{0.7}Ba_2Cu_3O_{7-\delta}$ (Pr0.7-O7), and $Y_{0.58}Pr_{0.42}Ba_2Cu_3O_{7-\delta}$ (Pr0.42-O7) single crystals in the temperature range 2–300 K with a field of 2000 G using a Quantum Design Superconducting quantum interference device (SQUID) magnetometer with field parallel (χ_c) and perpendicular ($\chi_{a,b}$) to the c axis. Paramagnetic anisotropy ($\Delta\chi$) was measured on $PrBa_2Cu_3O_6$ (Pr-O6) single crystals in the temperature range 77–300 K using a homemade torque magnetic anisotropy balance.[15]

III. THEORETICAL BACKGROUND

The structure of YPBCO consists of a Pr site with eight nearest oxygen neighbors in a nearly cubic configuration. The total Hamiltonian at the Pr^{3+} site is of the form

$$H=H_0+H_{\mathrm{CEF}}, \tag{1}$$

where H_0 represents the free-ion Hamiltonian consisting of the spherically symmetric one-electron part, the electrostatic repulsion between the equivalent f electrons, and the spin-orbit interaction. H_{CEF} represents the crystal-field part of the Hamiltonian, arising from the effect of the surrounding anions on the Pr^{3+} ion. Each $|J\rangle$ state of the free ion is $(2J+1)$-fold degenerate, and depending on the site symmetry of the Pr^{3+} in the crystal lattice, this degeneracy is lifted. In the case of Pr^{3+}, the intramultiplet splitting arising due to H_{CEF} has been found to be comparable to the intermultiplet splitting.[16–18] On account of this, it was found necessary to conduct the theoretical analysis taking into account J mixing of all 13 multiplets. Intermediate coupled wave functions were used during the calculations. The software developed for the present calculations has been described elsewhere.[19]

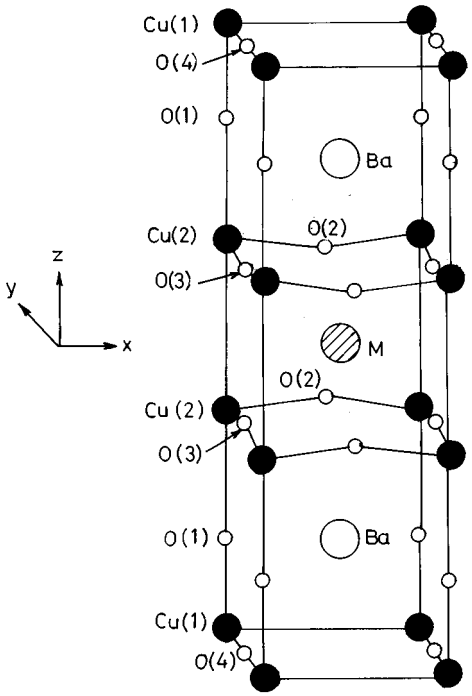

FIG. 1. Structural diagram of $Y_{1-x}Pr_xBa_2Cu_3O_{7-\delta}$ showing the various atomic coordinates.

The CF Hamiltonian at the Pr^{3+} site of YPBCO is of the form

$$H_{\mathrm{CEF}}=\sum_{k,q} B_k^q V_k^q, \tag{2}$$

where B's are the crystal-field parameters (CFP's) and V's are the n-particle unit irreducible spherical tensor operators. Here, $k=2,4,6$ and $q=0,2,4,6$ for orthorhombic symmetry. In the case of tetragonal site symmetry, k remains the same, but the terms with $q=2$ and 6 are absent. The matrix obtained on application of H_{CEF} was diagonalized to obtain the energy eigenvalues and the corresponding eigenfunctions. The magnetic perturbation $g_J\vec{H}\cdot\vec{J}$ was next applied on the CF levels to obtain expressions for the magnetic susceptibilities parallel (χ_c) and perpendicular ($\chi_{a,b}$) to the c axis using the Van Vleck formula.[9]

IV. RESULTS AND DISCUSSION

A. Structural

From our x-ray analysis on $PrBa_2Cu_3O_{7-\delta}$ (Pr-O7), the oxygen content after refinement was found to be 6.89. Pr-O7 was orthorhombic with space group $Pmmm$, $a=3.9132(5)$ Å, $b=3.9156(3)$ Å, and $c=11.7120(11)$ Å and $Z=1$. It was found that considering orthorhombicity with four inequivalent oxygen sites produced the best results. It is to be noted that O(4) is present only at the (0 1/2 0) site and not in the (1/2 0 0) site. The thermal parameters were unusually high when O(4) was considered to be only at the (1/2 0 0) site or when oxygen atoms were considered to be at both these sites.

TABLE I. Crystallographic data of $PrBa_2Cu_3O_{6.89}$ cells. Numbers in parentheses are standard deviations.

Atom	x	y	z	g^a	$U_{eq}(A^2)$
Pr	0.5	0.5	0.5	0.1250	15(1)
Ba	0.5	0.5	0.1853(2)	0.2500	20(1)
Cu(1)	0.0	0.0	0.0	0.1250	38(5)
Cu(2)	0.0	0.0	0.3517(4)	0.2500	17(2)
O(1)	0.0	0.0	0.1523(27)	0.2500	48(28)
O(2)	0.5	0.0	0.3761(23)	0.2500	15(1)
O(3)	0.0	0.5	0.3733(24)	0.2500	13(10)
O(4)	0.0	0.5	0.0	0.1122	118(87)

[a]Occupancy factor.

SHELX-93 enables more than two atoms to be assigned to a particular site, with the sum of site occupation factors restrained to be a constant. Also, the same isotropic or anisotropic displacement parameters are used for these two atoms. In the present case the sum of Y and Pr was restrained to be equal to 1 and refinement was performed. The YPBCO sample was found to be $Y_{0.58}Pr_{0.42}Ba_2Cu_3O_{6.78}$. The crystals were found to be tetragonal with space group $P4/mmm$, $a=3.877(5)$ Å, $b=3.877(5)$ Å, $c=11.692(3)$ Å and $Z=1$.

Figure 1 shows atom coordinates for $Y_{1-x}Pr_xBa_2Cu_3O_{7-\delta}$. Tables I and II list atom coordinates and equivalent thermal parameters for Pr-O7 and Pr0.42-O7, respectively. O(4) was isotropically refined in both the cases. The bond parameters of Pr-O6 (Ref. 9), Pr-O7, and Pr0.42-O7 are compared in Table III. Inspection of Table III shows significant differences in bond lengths with a shortening of Pr-O(2) and Cu(1)-O(1) in Pr-O7 compared to Pr-O6, which decreases further with a decrease in Pr content. The short Cu(1)-O(1) bond length indicates a higher oxidation state of Cu(1). A short Pr-O(2) bond length indicates an increased overlap between Pr and oxygen since the coordination number of oxygen around Pr remains the same from x-ray analysis. Further, there is no evidence of a Pr^{4+} from spectroscopic measurements, viz., photoemission,[20] x-ray absorption,[21] Raman,[22] and electron-energy-loss spectra.[23]

B. Magnetic susceptibilities and paramagnetic anisotropies

The room-temperature value of $\Delta\chi$ for Pr-O6 was found to be 5.6×10^{-4} emu/mol. The temperature variation of $\Delta\chi$ for Pr-O6 is shown in the inset of Fig. 2. In the case of Pr-O7, directional-susceptibility measurements were made taking precautions to reduce the background contributions. The paramagnetic anisotropy was determined from the difference of susceptibilities χ_c and $\chi_{a,b}$. The paramagnetic-anisotropy value of Pr-O7 at room temperature measured by the torque balance was found to be 7.4×10^{-4} emu/mol and that obtained from the SQUID magnetometer was found to be 7.1×10^{-4} emu/mol. On account of this agreement, the paramagnetic anisotropy in the case of Pr-O7 was obtained from the difference in the susceptibilities down to 2 K (Fig. 3, inset).

The paramagnetic anisotropy of YPBCO single crystals shows that $\chi_c>\chi_{a,b}$ at room temperature for all the compounds studied by us. Also $\chi_c>\chi_{a,b}$ throughout the temperature range of 300–2 K for Pr-O6 and Pr-O7. For compounds Pr0.7-O7 and Pr0.42-O7, it was found that $\chi_{a,b}>\chi_c$ below temperatures 110 and 60 K, respectively (Figs. 5 and 6, insets). In this context it may be mentioned that from neutron diffraction studies[2] the Pr spins were found to be aligned along the c axis around the ordering temperature for Pr-O7.

TABLE II. Crystallographic data of $Y_{0.58}Pr_{0.42}Ba_2Cu_3O_{6.78}$ cells. Numbers in parentheses are standard deviations.

Atom	x	y	z	g^a	$U_{eq}(A^2)$
Y	0.5	0.5	0.5	0.0625	2(1)
Pr	0.5	0.5	0.5	0.0625	2(1)
Ba	0.5	0.5	0.1856(1)	0.1250	5(1)
Cu(1)	0.0	0.0	0.0	0.0625	14(1)
Cu(2)	0.0	0.0	0.3544(2)	0.1250	3(1)
O(1)	0.0	0.0	0.1526(12)	0.1250	18(3)
O(2)	0.5	0.0	0.3751(7)	0.2500	5(2)
O(3)	0.0	0.5	0.3751(7)	0.2500	5(2)
O(4)	0.0	0.5	0.0	0.0495	14(11)

[a]Occupancy factor.

TABLE III. Bond lengths (Å) and bond angles (in degrees).

Atomic pair	Pr-O6	Pr-O7	Pr0.42-O7
Pr-O(2)	2.472(14)	2.437(6)	2.427(5)
Pr-O(3)	2.472(14)	2.456(6)	2.427(5)
Ba-O(1)	2.789(6)	2.795(4)	2.768(2)
Ba-O(2)	2.883(17)	2.971(20)	2.944(6)
Ba-O(3)	2.883(17)	2.946(21)	2.944(6)
Ba-O(4)	2.995(2)	2.922(2)	2.910(8)
Cu(1)-O(1)	1.848(38)	1.784(32)	1.785(14)
Cu(1)-O(4)	1.949(2)	1.958(0)	1.938(1)
Cu(2)-O(1)	2.341(39)	2.335(32)	2.359(14)
Cu(2)-O(2)	1.960(3)	1.977(4)	1.954(1)
Cu(2)-O(3)	1.960(3)	1.974(4)	1.954(1)
O(2)-Pr-O(3)	67.7(6)	68.9(3)	68.8(2)
O(2)-Pr-O(2)	76.1(6)	73.1(10)	74.0(3)

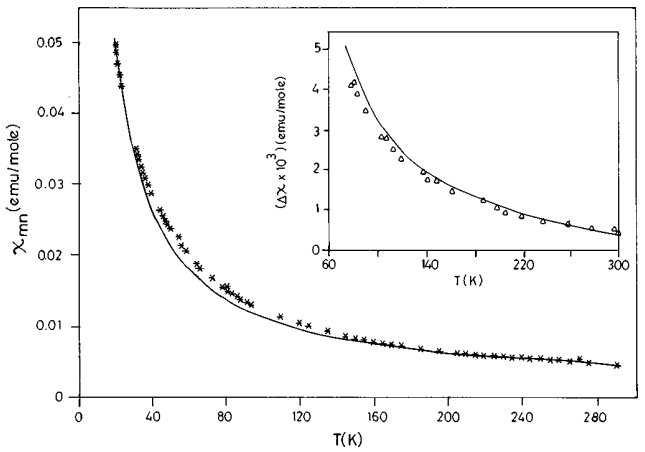

FIG. 2. Temperature variation of the mean magnetic susceptibility of $PrBa_2Cu_3O_6$: (*) experimental, (solid line) calculated. Inset: paramagnetic anisotropy ($\Delta\chi$) data of $PrBa_2Cu_3O_6$, (Δ) experimental, (solid line) calculated.

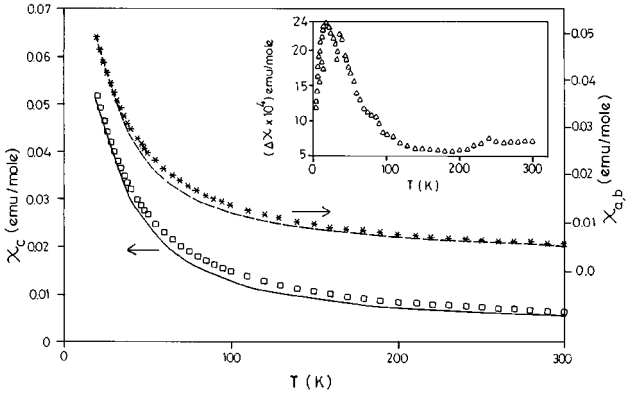

FIG. 3. Temperature variation of the directional magnetic susceptibilities of $PrBa_2Cu_3O_{6.89}$: (*,□) experimental and (dashed and solid lines) calculated values of $\chi_{a,b}$ and χ_c, respectively. Inset: paramagnetic anisotropy ($\Delta\chi$) of $PrBa_2Cu_3O_{6.89}$.

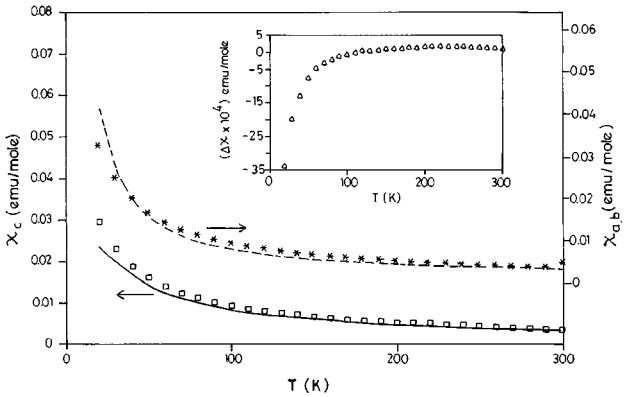

FIG. 5. Temperature variation of the directional magnetic susceptibilities of Pr0.7-O7: (*,□) experimental and (dashed and solid lines) calculated values of $\chi_{a,b}$ and χ_c, respectively. Inset: paramagnetic anisotropy ($\Delta\chi$) of Pr0.7-O7.

A decrease in the Pr concentration is expected to bring about a decrease in the number of Pr spins aligning along the c axis on lowering the temperature. This observation, however, is in contradiction to Jayaram *et al.*[10] who observed $\chi_c > \chi_{a,b}$ for all the concentrations studied by them throughout the temperature range of 5–300 K. It was also found by us that no measurable $\chi_a \sim \chi_b$ could be detected, and this is also evident from the crystal structure.

A superconducting transition was not observed for any of the four samples studied by us. It may be remarked that there is a gradual suppression of T_c with an increase in Pr content in the YPBCO system. Pr(0.4) is expected to show a typical T_c of 45 K as reported for the polycrystalline sample. Also, a comparison of T_c of single-crystal and polycrystalline samples would be valid only when the Pr and oxygen contents are the same in both cases. From our x-ray study on Pr0.42-O7, it has been found that the oxygen content is only 6.78. It is well known that oxygen content plays a vital role in determination of T_c. In single crystals it is difficult to incorporate oxygen to the desired value. Therefore this lower content of oxygen could have been a possible reason for our not having observed T_c for the sample Pr0.42-O7 and also by Jayaram *et al.*[10]

Magnetic ordering of praseodymium was observed by us in susceptibility measurements of Pr-O6 single crystals clearly showing a peak at 11.5 K reported in our earlier work (Fig. 4, inset), characteristic of antiferromagnetic ordering.[9] In the case of Pr-O7, the susceptibilities did not reveal any anomaly near 17 K. However, a peak was observed in $\Delta\chi$ at 17.5 K (Fig. 3, inset). This peak could be due to antiferromagnetic ordering of Pr. In this context it may be mentioned that Pr-O6 was grown in a platinum crucible[9] and Pr-O7 was grown in an alumina crucible. It is expected that Al substitutes for Cu in the chains and may cause suppression of T_N.[5] However, the present experimental findings show that alumina contamination has not altered T_N as reflected in $\Delta\chi$ values of Pr-O7 (Fig. 3, inset).

The inverse mean susceptibility of Pr-O6 clearly shows an anomaly around 230 K (Fig. 4). This could be due to the antiferromagnetic ordering of Cu^{2+}. Such an anomaly has also been observed in Pr-O7 around 240 K (Fig. 3, inset). Magnetic ordering of copper in polycrystalline Pr-O7 has been reported to be around 270 K from muon-spin-resonance (μSR) measurements.[24] Similar copper ordering in inverse-susceptibility measurements has also been reported for other compounds, viz., $Bi_2Sr_2PrCu_2O_8$.[25]

The crystal structure of Pr-O6 was found to be tetragonal even down to 4.2 K.[5] We therefore attempted a close fitting of the paramagnetic-anisotropy data by considering a CF of

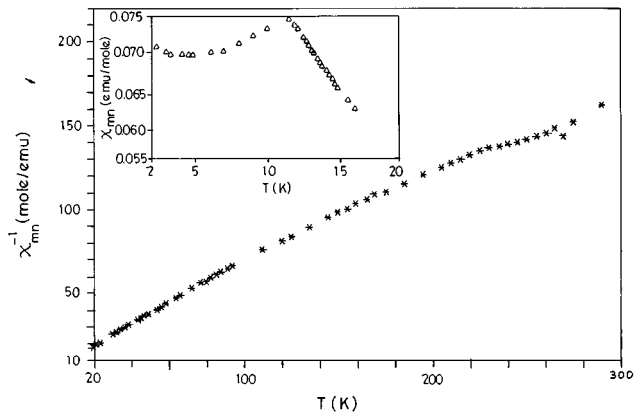

FIG. 4. Inverse experimental mean magnetic susceptibility of $PrBa_2Cu_3O_6$. Inset: antiferromagnetic ordering in $PrBa_2Cu_3O_6$.

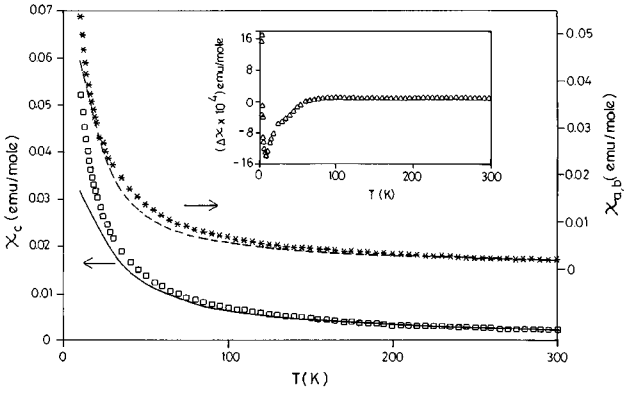

FIG. 6. Temperature variation of the directional magnetic susceptibilities of Pr0.42-O7: (*,□) experimental and (dashed and solid lines) calculated values of $\chi_{a,b}$ and χ_c, respectively. Inset: paramagnetic anisotropy ($\Delta\chi$) of Pr0.42-O7.

tetragonal symmetry. At the outset, we attempted to fit the paramagnetic anisotropy ($\Delta\chi$) by substituting the values of the CFP's reported in earlier work on inelastic neutron scattering.[4–6] It was, however, observed that the corresponding temperature dependence of the paramagnetic anisotropy could not satisfactorily account for the room temperature as well as the temperature variation of the experimental values of $\Delta\chi$.

Therefore each of the crystal-field parameters was varied so as to study the actual effect of a particular CFP in different temperature intervals. In this manner the CFP's were varied so as to obtain agreement between the calculated paramagnetic-anisotropy value and the experimental value. It was noticed that in order to get a good fit of $\Delta\chi$ at room temperature the variation of B_2^0 was crucial. Likewise, it was also seen that B_4^0 played a major role in adjusting the rate of increase of $\Delta\chi$ on lowering the temperature.

We next attempted a fit to our experimental results on χ_{mn} and $\Delta\chi$ by a variation of the crystal-field parameters which would also maintain the INS energy levels nearly unchanged. In this context it may be mentioned that the Pr^{3+} contribution to the susceptibility was determined by the following method:

$$\chi_{mn}(Pr^{3+}) = \chi_{mn} - \chi_{Cu} - \chi_0 . \tag{3}$$

Here χ_{Cu} is the copper contribution to the susceptibility and is determined by measuring the susceptibility of $YBa_2Cu_3O_6$. χ_0 has been determined from an initial Curie-Weiss law fit to the experimental data.

It was found that during the fitting procedure even small changes (± 1 cm^{-1}) in the values of the crystal-field parameters brought about large variations ($\pm 5\times10^{-5}$ emu/mol) even though the energy-level pattern was found not to show any detectable changes. The temperature variation of the calculated values of the paramagnetic anisotropy and mean susceptibility along with the actual experimental results of Pr-O6 are shown in Fig. 2.

TABLE IV. Crystal-field parameters in cm^{-1} of Pr-O6, Pr-O7, Pr0.42-O7, and Pr0.7-O7 in n-particle unit irreducible spherical tensor notation.

B_k^q	Pr-O6	Pr-O7	Pr0.42-O7	Pr0.7-O7
B_2^0	215	−500	120	250
B_2^2		−270		
B_4^0	−3494	−3355	−3654	−3654
B_4^2		−600		
B_4^4	1375	1652	1322	1302
B_6^0	−1020	−1310	−1160	−1160
B_6^2		−125		
B_6^4	−2050	−2895	−2806	−2895
B_6^6		−10	180	80

Results of the magnetic susceptibility of Pr-O7 were initially analyzed considering only tetragonal CF parameters since the lattice parameters are nearly tetragonal. In spite of our repeated trials, it was not possible to get a good fit to our data. Small values of the CF parameters B_2^2, B_4^2, and B_6^2 had to be incorporated to fit the experimental results. It was found that B_6^6 is a crucial parameter in accounting for the low-lying energy-level scheme. In general, B_2^0 and B_2^2 are parameters which have a strong influence on the energy lev-

TABLE V. CF energy levels and wave function compositions appropriate to the ground multiplet of $PrBa_2Cu_3O_6$ and $PrBa_2Cu_3O_{6.89}$ in a 91-level CF calculation. [a] Experimental values (after Refs. 5 and 6) are shown in parentheses.

CF levels (meV)	Wave functions
0	$0.2753\|4,\pm1\rangle + 0.9601\|4,\mp3\rangle$
0 [b]	$0.6616\|4,-3\rangle + 0.2451\|4,-1\rangle + 0.2451\|4,1\rangle + 0.6616\|4,3\rangle$
(1.5) [b]	
1.5(1.7)	$0.7064\|4,-2\rangle + 0.7064\|4,2\rangle$
3.9(3.3) [b]	$-0.1035\|4,-4\rangle + 0.6835\|4,-2\rangle + 0.2007\|4,0\rangle + 0.6835\|4,2,\rangle - 0.1035\|4,4\rangle$
(3.4)	
(4.8)	
4.7(4.8) [b]	$-0.6910\|4,-3\rangle + 0.1396\|4,-1\rangle - 0.1396\|4,1\rangle + 0.6910\|4,3\rangle$
61.0 [b]	$-0.6665\|4,-4\rangle + 0.1524\|4,-2\rangle - 0.1524\|4,2\rangle + 0.6665\|4,4\rangle$
62.6(61.5)	$0.6883\|4,-2\rangle - 0.6883\|4,2\rangle$
62.0(63.0) [b]	$0.6099\|4,-4\rangle + 0.1567\|4,-2\rangle - 0.4316\|4,0\rangle + 0.1567\|4,2\rangle + 0.6099\|4,4\rangle$
65.5(65.2)	$0.9428\|4,\mp1\rangle - 0.2685\|4,\pm3\rangle$
67.4(67.8) [b]	$-0.2366\|4,-3\rangle + 0.6369\|4,-1\rangle + 0.6369\|4,1\rangle - 0.2366\|4,3\rangle$
68.1	$-0.3608\|4,-4\rangle + 0.8546\|4,0\rangle - 0.3608\|4,4\rangle$
77.3(76.0)	$-0.6862\|4,-4\rangle + 0.6862\|4,4\rangle$
84.5(83.0) [b]	$0.1562\|4,-4\rangle + 0.6619\|4,-2\rangle - 0.6619\|4,2\rangle - 0.1562\|4,4\rangle$
84.5(84.7)	$0.5877\|4,-4\rangle + 0.4936\|4,0\rangle + 0.5877\|4,4\rangle$
89.5 [b]	$0.1294\|4,-3\rangle + 0.6721\|4,-1\rangle - 0.6721\|4,1\rangle - 0.1294\|4,3\rangle$
98.8(97.4) [b]	$0.3083\|4,-4\rangle - 0.0831\|4,-2\rangle + 0.8544\|4,0\rangle - 0.0831\|4,2\rangle + 0.3083\|4,4\rangle$

[a] Detailed wave function table available from authors.

[b] Levels due to $PrBa_2Cu_3O_{7-\delta}$.

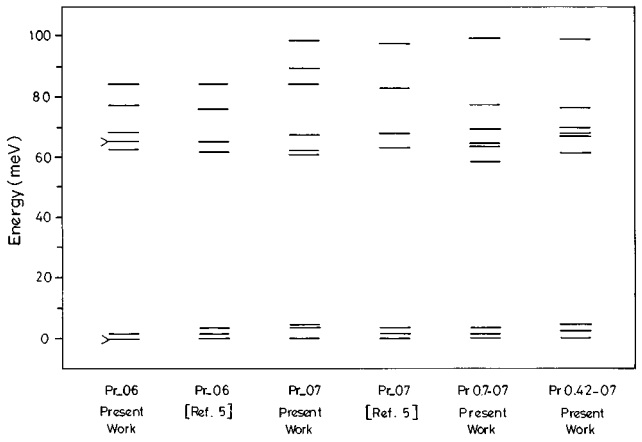

FIG. 7. CF energy-level diagram of $Y_{1-x}Pr_xBa_2Cu_3O_{7-\delta}$ in meV.

els as well as the susceptibilities. The calculated and experimental directional susceptibilities are shown in Fig. 3. The best set of CF parameters and the corresponding CF energy level pattern along with the wave functions for Pr-O6 and Pr-O7 are given in Tables IV and V, respectively.

A similar CF analysis was undertaken so as to theoretically account for the magnetic susceptibilities of Pr0.7-O7 and Pr0.42-O7. The best-fitted CF parameters are shown in Table IV. Since the INS spectra are not available for both these compositions, it has not been possible to compare the entire spectrum of the $^3H_4$ multiplet. However, the low-lying level patterns for both these compositions vary only slightly from Pr-O7 as reported by Jostarndt *et al.*[26] The calculated values of the magnetic susceptibilities together with the experimental data for Pr0.7-O7 and Pr0.42-O7 are shown in Figs. 5 and 6, respectively. The energy levels of the various compositions studied by us together with the INS data are shown in Fig. 7. It may be mentioned here that the magnetic susceptibilities and/or paramagnetic anisotropy of all the compounds studied by us could be explained satisfactorily by considering a CF calculation based on Pr^{3+} alone.

The present analysis of the experimental data through CF theory considering Pr^{3+} ions only is able to account for the magnetic susceptibility and its anisotropy and INS data fairly well. The larger values of the CFP's of Pr-O7 compared to Pr-O6 show that the CF interaction is stronger in Pr-O7. This is also evident from our x-ray analysis where we find that the bond length of Pr-O7 is shorter than in Pr-O6. A prominent difference between the CFP's of Pr-O6 and Pr-O7 is that there is a sign change in B_2^0. Also, there are slight differences in the energy-level scheme.

During our fitting procedure, it was found that J mixing was essential to fit the directional susceptibilities, paramagnetic anisotropy, and the INS data well. For example, in the case of Pr-O6, the width of the ground multiplet corresponds to an overall splitting of 103.5, 91.7, 91.8, and 84.5 meV for 9-, 20-, 33-, and 91-level fits, respectively. The observed overall splitting of the ground multiplet of Pr-O6 is 84.7 meV.[5] Similarly the paramagnetic anisotropy at 100 K is found to be 2.79×10^{-3}, 3.03×10^{-3}, 3.04×10^{-3}, and 3.14×10^{-3} emu/mol for 9-, 20-, 33-, and 91-level fits, respectively.

It is interesting to mention here that the INS spectra of Pr-O6 (Ref. 5) above 30 K clearly show a two-level low-lying level pattern as obtained from the present calculations. However, below T_N a quasitriplet is clearly noticed with CF lines at 1.7 and 3.4 meV, although x-ray analysis of this compound shows a tetragonal structure even down to 4.2 K.[5] This could probably be an effect of magnetic ordering and/or Jahn-Teller effect normally observed in praseodymium systems.[27]

In conclusion, it may be remarked that the present set of CFP's is able to explain fairly well a number of physical properties, viz., paramagnetic anisotropy, mean magnetic susceptibility, and the CF levels as reported from inelastic neutron scattering spectra.

ACKNOWLEDGMENTS

Financial support from the National Superconductivity Board-Department of Science and Technology, India was gratefully acknowledged. T.S. and K.S. thank the Council for Scientific and Industrial Research, Government of India, for support. Thanks are also due to Dr. Babu Varghese for the x-ray data.

[1] A. Kebede, C. S. Jee, J. Schwegler, J. E. Crow, T. Mihalisin, G. Myer, R. E. Salomon, P. Schlottman, M. V. Kuric, S. H. Bloom, and R. P. Guertin, Phys. Rev. B **40**, 4453 (1989).

[2] W. H. Li, J. W. Lynn, S. Skanthakumar, T. W. Clinton, A. Kebede, C. S. Jee, J. E. Crow, and T. Mihalisin, Phys. Rev. B **40**, 5300 (1989).

[3] M. Guillaume, P. Fischer, B. Roessli, A. Podlesnyak, J. Schefer, and A. Furrer, Solid State Commun. **88**, 57 (1993).

[4] L. Soderholm, C. K. Loong, G. L. Goodman, and B. D. Debrowski, Phys. Rev. B **43**, 7923 (1991).

[5] G. Hilscher, E. Holland-Moritz, T. Holubar, H. D. Jostarndt, V. Nekvasil, G. Schaudy, U. Walter, and G. Fillion, Phys. Rev. B **49**, 535 (1994).

[6] A. T. Boothroyd, S. M. Doyle, and R. Osborn, Physica C **217**, 425 (1993).

[7] E. Moran, U. Amador, M. Barahona, M. A. Alario-Franco, A. Vegas, and J. Rodriguex-Caravajal, Physica C **153-155**, 423 (1988).

[8] G. Collin, P. A. Albouy, P. Monod, and M. Ribault, J. Phys. **51**, 1163 (1990).

[9] S. Uma, T. Sarkar, M. Seshasayee, G. Rangarajan, C. R. Venkateswara Rao, and C. Subramanian, Solid State Commun. **87**, 289 (1993).

[10] B. Jayaram, H. Srikanth, B. M. Wanklyn, C. Changkang, E. Hllzinger-Schwieger, and G. Leising, Phys. Rev. B **52**, 89 (1995).

[11] Chen Changkang, Hu Yongle, B. M. Wanklyn, S. Hazell, A. K. Pradhan, J. W. Hodby, A. Boothroyd, and F. R. Wondre, J. Cryst. Growth **128**, 767 (1993).

[12] Changkang Chen, J. W. Hodby, Yongle Hu, and B. M. Wanklyn, J. Mater. Chem. **4**, 469 (1994).
[13] F. Ugozzoli, Comput. Chem. **11**, 109 (1987).
[14] G. M. Sheldrick, Computer Code SHELX-93, program for the refinement of crystal structures, Institut für Anorganic Chemie, Götingen, Germany, 1993.
[15] T. Kundu, S. Dasgupta, M. Saha, and D. Ghosh, Ind. J. Phys. **60A**, 312 (1986).
[16] R. Sarup and M. H. Crozier, J. Chem. Phys. **42**, 371 (1965).
[17] J. B. Gruber, J. Chem. Phys. **38**, 946 (1963).
[18] N. H. Kiess and G. H. Dieke, J. Chem. Phys. **45**, 2729 (1966).
[19] Nithya Ravindran, T. Sarkar, S. Uma, G. Rangarajan, and V. Sankaranarayanan, Phys. Rev. B **52**, 7656 (1995).
[20] J. S. Kang, J. W. Allen, Z. X. Shen, W. P. Ellis, J. J. Yeh, B. W. Lee, M. B. Maple, W. E. Spicer, and I. Lindau, J. Less-Common Met. **148**, 121 (1989).
[21] L. Soderholm and G. L. Goodman, J. Solid State Chem. **81**, 121 (1989).
[22] R. Bhadra, T. O. Brun, M. A. Beno, B. Dabrowski, D. G. Hinks, L. S. Liu, J. D. Jorgenson, L. J. Nowicki, A. P. Paulikas, I. K. Schuller, C. U. Segre, L. Soderholm, B. Veal, H. H. Wang, J. M. Williams, K. Zhang, and M. Grimsditch, Phys. Rev. B **37**, 5142 (1988).
[23] J. Fink, N. Nucker, H. Romberg, and M. Alexander, Phys. Rev. B **42**, 4823 (1990).
[24] D. W. Cooke, R. S. Kwok, R. L. Lichti, T. R. Adams, C. Boekema, W. K. Dawson, A. Kebede, J. Schwegler, J. E. Crow, and T. Mihalisin, Phys. Rev. B **41**, 4801 (1990).
[25] V. P. S. Awana, Latika Menon, and S. K. Malik, Phys. Rev. B **51**, 9379 (1995).
[26] H.-D. Jostarndt, U. Walter, J. Harnischmacher, J. Kalenborn, A. Severing, and E. Holland-Moritz, Phys. Rev. B **46**, 14 872 (1992).
[27] D. R. Taylor, J. P. Harrison, and D. B. McColl, Physica **86-88B**, 1164 (1977).